Korean Journal of Nuclear Medicine Technology, Volume 30, Number 2, Article 24, November 2026.
Korean J Nucl Med Technol 2026;30(2):24. https://doi.org/10.12972/kjnmt.2026.30.2.24
pISSN 1229-9901
eISSN 2982-8406

Original article

금속 삽입물 환자에서 iMAR 알고리즘 적용에 따른 CT 및 PET 영상의 변화 분석

김지현, 방사선사, 류재광, 방사선사, 백수호, 방사선사
서울아산병원 핵의학과

Analysis of Image Quality on CT and PET following the Application of the iMAR Algorithm in Patients with Metallic Implants

Ji-Hyeon Kim, Radiological Technologist, Jae-Kwang Ryu, Radiological Technologist and Su-Ho Beak, Radiological Technologist
Department of Nuclear Medicine, Asan Medical Center, Seoul, Korea

Corresponding Author: Jae-Kwang Ryu, Department of Nuclear Medicine, Asan Medical Center, 88, Olympic-ro 43-gil, Songpa-gu, Seoul, 05505, Republic of Korea. Tel: +82-2-3010-5421, E-mail: huhjoon11@naver.com

Abstract

Purpose: Metallic implants can lead to metal artifacts in PET/CT imaging, which may affect CT-based attenuation correction and PET quantification. The aim of this study was to evaluate differences in quantitative parameters of CT and PET images following the application of implant-specific iMAR(Iterative Metal Artifact Reduction) algorithms. **Materials and Methods**: This retrospective study included 81 patients who underwent ^{18}F-FDG PET/CT scans; it analyzed a total of 90 cases of metallic implants. Representative CT and PET images before and after iMAR application were compared visually. For quantitative analysis, CT HU_{mean}, PET SUV_{mean}, and SUV_{max} were measured, while liver SUV_{mean} was assessed separately. **Results**: A visual comparison of the representative images showed that the metal artifacts decreased in CT images after iMAR application, but no obvious visual differences were observed in PET images. In the quantitative analysis, for all three implant types, CT HU_{mean}, PET SUV_{mean}, and SUV_{max} in the bright band regions decreased significantly after iMAR application, while they increased significantly in the dark band regions. In contrast, no statistically significant differences were observed in liver SUV_{mean}. **Conclusion**: Implant-specific iMAR application resulted in significant differences in CT HU_{mean}, PET SUV_{mean}, and SUV_{max} in metal artifact regions. These results suggest that the reconstruction conditions of CT images used for PET attenuation correction may affect the PET quantification values around the metal artifact area. Therefore, when interpreting the quantitative values of areas adjacent to metal in PET/CT images, the application of iMAR must be considered.

Keywords: PET/CT, iMAR, Metal Artifact, HU(Hounsfield Unit), SUV(Standardized Uptake Value)

Received November 02, 2026 **Revised** November 13, 2026 **Accepted** November 16, 2026

This is an Open Access article distributed under the terms of the Creative Commons CC BY 4.0 license (https://creativecommons.org/licenses/by/4.0/) which permits unrestricted use, distribution, and reproduction in any medium, provided the original work is properly cited.

Introduction

PET/CT(Positron Emission Tomography/Computed Tomography) is an imaging modality that combines metabolic information from PET with anatomical information from CT; it is used to locate lesions and assess metabolic activity, among other applications[1]. To ensure the quantitative accuracy of PET images, it is essential to accurately correct for the attenuation of annihilation photons as they pass through tissue within the body. In PET/CT, an attenuation map(μ-map) is generated using information obtained from CT images, and this map is applied to the acquired PET images as attenuation correction(AC)[1]. Therefore, artifacts present in the CT images affect the creation of the attenuation map and can potentially cause quantitative errors in the PET images[1,2,14]. Metallic implants can lead to metal artifacts appearing as bright and dark streaks in CT images, which can distort the Hounsfield Unit(HU) values of surrounding tissues and degrade image quality[3,4]. When HU values in CT images are distorted, the attenuation coefficient may be over or under estimated, leading to quantitative errors in tracer uptake around the metal artifact area[1,2]. Therefore, reducing metal artifacts is important in PET/CT imaging. Nowadays, various metal artifact reduction(MAR) techniques have been developed to mitigate these metal artifacts[2,3]. Conventional projection-data-based MAR techniques interpolate regions of projection data affected by metal using surrounding data. However, these methods have limitations, as they may result in the loss of anatomical information or the generation of new artifacts[5].

To address this issue, Normalized Metal Artifact Reduction(NMAR) was proposed as a method that reduces the generation of new artifacts through the normalization and interpolation of projection data using a prior image[5]. Frequency Split Metal Artifact Reduction(FSMAR), proposed in conjunction with NMAR, is a method that combines the low-frequency components of the corrected image with the high-frequency components of the original image to reduce metal artifacts while preserving anatomical details[6]. Iterative Metal Artifact Reduction(iMAR), which combines the principles of these two techniques, is an algorithm that reduces residual metal artifacts by repeatedly performing projection data correction and combining image information. Furthermore, different iMAR algorithms can be applied depending on the type of metallic implant[7]. The effectiveness of metal artifact reduction techniques has been reported in several previous studies[15]. The application of iMAR has improved the quality of CT images around metallic implants[8], and reductions in quantitative errors resulting from PET AC, as well as differences in quantitative parameters, have also been reported[9,11]. However, another study reported that while HU values in CT images changed significantly after applying iMAR, no significant differences were observed in Standardized Uptake Value(SUV) values in PET images[10]. Previous studies have evaluated particular implant types or phantom models[8-11]. Therefore, there is a need to further evaluate differences in CT and PET quantitative parameters resulting from the application of iMAR across various types of metallic implants.

Therefore, this study aimed to evaluate differences in quantitative parameters in CT and PET images before and after applying the iMAR algorithm to patients with dental fillings, spine implants, and hip implants, corresponding to each type of metallic implant. Through this, we sought to confirm the effect of iMAR application on CT and PET images around metallic implants and to provide foundational data necessary for interpreting quantitative values around metallic implants in PET/CT examinations.

Materials and Methods

1. Study Population

This retrospective study included 81 patients(50 men and 31 women) with metallic implants who underwent ^{18}F-FDG PET/CT scans at a single institution. The analysis included a total of 90 cases: 35 dental fillings, 32 spinal implants, and 23 hip implants. Patients with two or more types of metallic implants were included in the analysis for each respective implant type.

2. Image Acquisition and Reconstruction

PET/CT images were acquired using a Biograph Vision 600(Siemens Healthineers, Germany). The CT tube voltage was set to 120 kVp and Auto mA control was applied. Using previously acquired CT raw data, we reconstructed both the original CT images and iMAR-reconstructed CT images corresponding to the type of metallic implant. The Dental Filling iMAR algorithm was applied to dental prostheses, the Spine Implant iMAR algorithm to spinal fixation devices, and the Hip Implant iMAR algorithm to hip replacements. Subsequently, the original CT and iMAR-reconstructed CT images were separately used for AC to reconstruct the corresponding PET images.

3. Image Comparison and Quantitative Analysis

We qualitatively compared representative CT and PET images for each type of metallic implant to examine the differences in metal artifacts before and after iMAR application and to assess visual differences. For quantitative analysis, regions of interest(ROIs) each measuring 0.5 cm^2 were placed in the bright band and dark band regions surrounding the metal area in the CT images, and HU_{mean} was measured(Fig. 1A, 1B). The ROIs were placed within the artifact-affected regions, excluding the implanted metal itself, and were positioned at the same cross-section and location on both the original CT and the iMAR-reconstructed CT images for the same patient. For PET images, ROIs of the same location and size as those in the CT images were defined to measure SUV_{mean} and SUV_{max}(Fig. 1C, 1D). Additionally, liver SUV_{mean} was measured to provide a comparison with normal tissue unaffected by metal artifacts[12].

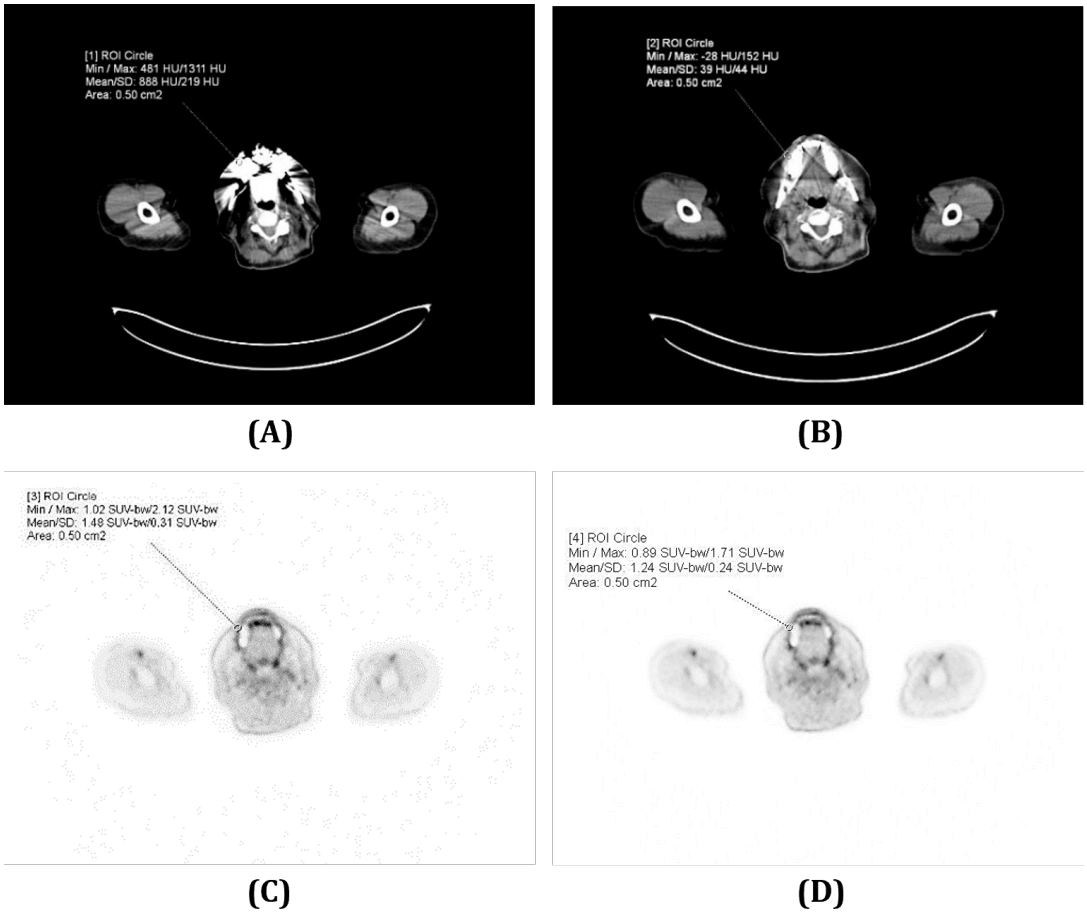


Fig. 1. Representative CT and PET images illustrating ROI placement in the bright band artifact region of a patient with a dental filling. (A) Original CT image. (B) iMAR CT image. (C) PET AC image using the original CT. (D) PET AC image using the iMAR CT. A 0.5 cm^2 ROI was placed at the same location in all four images.

4. Statistical Analysis

To compare differences in quantitative parameters before and after iMAR application, paired comparisons were performed for each metallic implant type. A paired t-test was used for the Dental Filling and Spine Implant groups, while the Wilcoxon signed-rank test was used for the Hip Implant group. The statistical significance level was set at $p<0.05$.

Results

1. Comparison of CT HU_{mean}

A visual comparison of representative CT images for each type of metallic implant revealed that, for all three types, the presence of bright and dark band-shaped artifacts around the metal area decreased after applying iMAR(Fig. 2). A comparison of the HU_{mean} values in the CT images showed that, for all three types, the HU_{mean} decreased in the bright band regions and increased in the dark band regions. The HU_{mean} in the bright band regions decreased from 564.29 HU to 50.03 HU for dental fillings, from 305.41 HU to 75.31 HU for spine implants, and from 548.13 HU to 102.57 HU for hip implants. In contrast, in the dark band regions, the values increased from -501.11 HU to 10.17 HU, from -257.12 HU to -81.16 HU, and from -578.96 HU to 39.78 HU, respectively. These differences were statistically significant in all comparisons within three types of metallic implants(Table 1).

Table 1. Statistical analysis of CT HU_{mean} before and after iMAR by metallic implant type

Implant type	Artifact Area	Original CT (mean ± sd)	iMAR CT (mean ± sd)	t / z	p-value
Dental Filling (n=35)	Bright Band	564.29 ± 230.44	50.03 ± 65.87	11.9	< 0.001
	Dark Band	-501.11 ± 183.99	10.17 ± 77.37	-13.9	< 0.001
Spine Implant (n=32)	Bright Band	305.41 ± 200.26	75.31 ± 105.23	9.9	< 0.001
	Dark Band	-257.12 ± 128.14	-81.16 ± 64.49	-8.0	< 0.001
Hip Implant (n=23)	Bright Band	548.13 ± 188.57	102.57 ± 47.15	-4.2	< 0.001
	Dark Band	-578.96 ± 240.04	39.78 ± 43.55	-4.2	< 0.001

2. Comparison of PET SUV_{mean} and SUV_{max}

In representative PET images for each type of metallic implant, no visually distinct differences were observed before and after iMAR application(Fig. 2). A comparison of quantitative PET image parameters revealed that, for all three types of metallic implants, SUV_{mean} and SUV_{max} decreased in the bright band regions and increased in the dark band regions.

In the bright band regions, SUV_{mean} decreased from 1.172 to 1.083 for dental fillings, from 1.048 to 1.005 for spine implants, and from 0.934 to 0.879 for hip implants. In contrast, in the dark band regions, they increased from 1.113 to 1.230, from 0.651 to 0.688, and from 0.989 to 1.149, respectively(Table 2). In the bright band regions, SUV_{max} decreased from 1.653 to 1.525 for dental fillings, from 1.315 to 1.262 for spine implants, and from 1.227 to 1.159 for hip implants. In contrast, in the dark band region, they increased from 1.448 to 1.607, 0.871 to 0.907, and 1.323 to 1.530, respectively(Table 3). The differences in SUV_{mean} and SUV_{max} before and after application were statistically significant for all types of metallic implants.

Table 2. Statistical analysis of PET SUV_{mean} before and after iMAR by metallic implant type

Implant type	Artifact Area	Original PET (mean ± sd)	iMAR PET (mean ± sd)	t / z	p-value
Dental Filling	Bright Band	1.17 ± 0.53	1.08 ± 0.49	5.7	< 0.001
(n=35)	Dark Band	1.11 ± 0.73	1.23 ± 0.80	-6.9	< 0.001
Spine Implant	Bright Band	1.05 ± 0.48	1.00 ± 0.46	7.0	< 0.001
(n=32)	Dark Band	0.65 ± 0.36	0.69 ± 0.40	-3.5	0.001
Hip Implant	Bright Band	0.93 ± 0.47	0.88 ± 0.45	-4.2	< 0.001
(n=23)	Dark Band	0.99 ± 0.61	1.15 ± 0.72	-4.2	< 0.001

Table 3. Statistical analysis of PET SUV_{max} before and after iMAR by metallic implant type

Implant type	Artifact Area	Original PET (mean ± sd)	iMAR PET (mean ± sd)	t / z	p-value
Dental Filling	Bright Band	1.65 ± 0.70	1.53 ± 0.65	5.2	< 0.001
(n=35)	Dark Band	1.45 ± 0.84	1.61 ± 0.94	-6.8	< 0.001
Spine Implant	Bright Band	1.32 ± 0.69	1.26 ± 0.66	6.9	< 0.001
(n=32)	Dark Band	0.87 ± 0.56	0.91 ± 0.59	-5.0	< 0.001
Hip Implant	Bright Band	1.23 ± 0.62	1.16 ± 0.61	-4.1	< 0.001
(n=23)	Dark Band	1.32 ± 0.76	1.53 ± 0.91	-4.2	< 0.001

3. Comparison of SUV_{mean} in Normal Tissue

The SUV_{mean} of the liver—normal tissue distant from metallic implants—decreased slightly from 2.181 to 2.178 for dental fillings, from 2.161 to 2.157 for spine implants, and from 2.015 to 2.013 for hip implants. No statistically significant differences were observed for dental fillings or spine implants, and the Wilcoxon signed-rank test also revealed no significant difference for hip implants(Table 4).

Table 4. Statistical analysis of liver SUV_{mean} before and after iMAR by metallic implant type

Implant type	Original PET (mean ± sd)	iMAR PET (mean ± sd)	t / z	p-value
Dental Filling (n=35)	2.18 ± 0.32	2.18 ± 0.32	1.4	0.176
Spine Implant (n=32)	2.16 ± 0.42	2.16 ± 0.41	1.5	0.126
Hip Implant (n=23)	2.02 ± 0.36	2.01 ± 0.36	-1.3	0.172

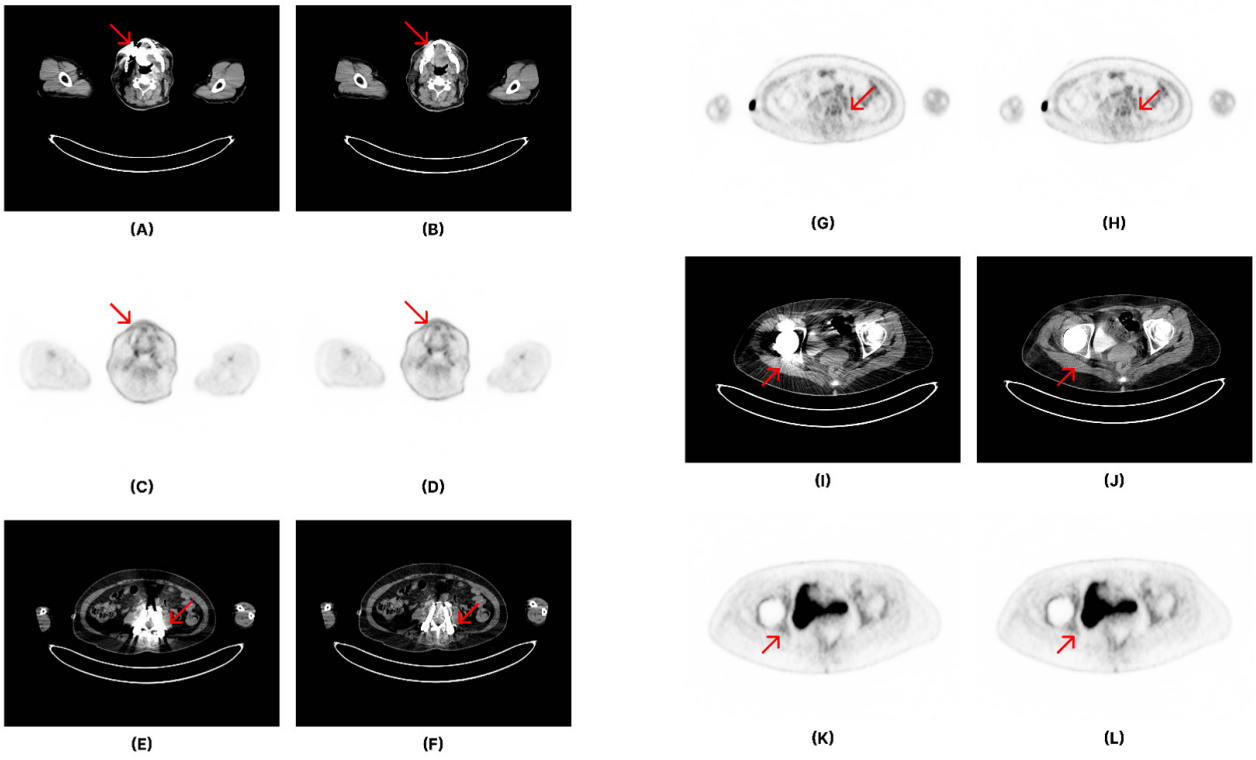


Fig. 2. Representative CT and PET images before and after iMAR application according to metallic implant type. (A–D) Dental filling, (E–H) Spine implant, and (I–L) Hip implant. Original CT images are shown in (A, E, I), iMAR CT images in (B, F, J), PET AC images using original CT in (C, G, K), and PET AC images using iMAR CT in (D, H, L). Red arrows indicate regions of metal artifacts in the CT images before and after iMAR application.

Discussion

In this study, following the application of iMAR, both CT HU and PET SUV decreased in bright band regions and increased in dark band regions for all three types of metallic implants. These results suggest that reducing metal artifacts during the CT reconstruction process also affects the information used for PET AC, and that PET quantitative values around metal artifact area may vary depending on the CT reconstruction conditions. While previous studies have reported improvements in CT image quality and reductions in PET quantitative errors following the application of iMAR[8,9], other studies found no significant differences in PET SUV despite significant differences in CT HU[10,13]. In contrast, SUV values around the metal artifact area changed significantly for all three types of metallic implants. However, these differences must be interpreted in light of the varying study conditions, such as the type of metallic implant and the region of interest[10,13]. Differences in SUV near metallic implants following iMAR application were statistically significant, with absolute percentage changes ranging from 4.1 to 16.2% for SUV_{mean} and 4.0 to 15.6% for SUV_{max}. Statistical significance does not necessarily imply clinically meaningful differences; the impact of these SUV differences on lesion interpretation and clinical decision-making requires further evaluation. Therefore, when interpreting PET quantitative values around metal artifact area, it is necessary to consider the reconstruction conditions of the CT images used for AC. Furthermore, these differences in quantitative values do not necessarily indicate an improvement in PET quantification accuracy. Nevertheless, providing PET images reconstructed using iMAR CT for AC alongside conventional PET images may offer additional information for image interpretation, similar to the complementary use of non-AC PET images.

Since this study did not compare results to a baseline without metal artifacts, it was not possible to determine whether the application of iMAR improved accuracy. Furthermore, because only the iMAR algorithm corresponding to each type of metallic implant was applied, a direct comparison of performance among algorithms was not possible; there is also the possibility of measurement variability due to residual artifacts and the location of the ROI. As this was a retrospective study conducted at a single institution using PET/CT equipment from a specific manufacturer, there are limitations to the generalizability of the results. In addition, previous studies have reported that increasing CT tube voltage can reduce metal artifacts[16]. Therefore, future studies should consider varying CT acquisition parameters, evaluate PET quantification accuracy using reference values without metallic artifacts and further examine the effects of ROI placement and reconstruction conditions.

Conclusion

In this study, we examined qualitative findings and quantitative parameters in CT and PET images before and after the application of iMAR in patients with metallic artifact. In the CT images, a reduction in bright and dark band-like artifacts around the metal area was observed after iMAR application; however, no obvious visual differences were observed in the PET images. However, significant differences were observed in the quantitative PET parameters(SUV_{mean}, SUV_{max}) around the metal artifact area. In contrast, no differences were observed in liver SUV_{mean}, as a measured in normal tissue. In CT images within metal artifact can affect PET AC, potentially altering quantitative values around the metal artifact area. Therefore, when interpreting quantitative values in regions adjacent to metal on PET/CT images following the application of iMAR, it is necessary to also consider whether iMAR was applied to the CT images used for AC.

References

1. Kinahan PE, Hasegawa BH, Beyer T. X-ray-based attenuation correction for positron emission tomography/computed tomography scanners. Semin Nucl Med. 2003;33(3):166-79. DOI: https://doi.org/10.1053/snuc.2003.127307.
2. Abdoli M, Dierckx RAJO, Zaidi H. Metal artifact reduction strategies for improved attenuation correction in hybrid PET/CT imaging. Med Phys. 2012;39(6):3343-60. DOI: https://doi.org/10.1118/1.4709599.
3. Katsura M, Sato J, Akahane M, Kunimatsu A, Abe O. Current and novel techniques for metal artifact reduction at CT: Practical guide for radiologists. Radiographics. 2018;38(2):450-61. DOI: https://doi.org/10.1148/rg.2018170102.
4. Barrett JF, Keat N. Artifacts in CT: Recognition and avoidance. Radiographics. 2004;24(6):1679-91. DOI: https://doi.org/10.1148/rg.246045065.
5. Meyer E, Raupach R, Lell M, Schmidt B, Kachelriess M. Normalized metal artifact reduction (NMAR) in computed tomography. Med Phys. 2010;37(10):5482-93. DOI: https://doi.org/10.1118/1.3484090.
6. Meyer E, Raupach R, Lell M, Schmidt B, Kachelriess M. Frequency split metal artifact reduction (FSMAR) in computed tomography. Med Phys. 2012;39(4):1904-16. DOI: https://doi.org/10.1118/1.3691902.
7. Kachelrieß M, Krauss A. Iterative metal artifact reduction (iMAR): Technical principles and clinical results in radiation therapy. Siemens Healthcare GmbH. 2021. Germany. White paper. Available at: https://www.siemens-healthineers.com/en-us/radiotherapy/ct-for-rt/somatom-go-platform/imar-white-paper
8. Wuest W, May MS, Brand M, Bayerl N, Krauss A, Uder M, et al. Improved image quality in head and neck CT using a 3D iterative approach to reduce metal artifact. AJNR Am J Neuroradiol. 2015;36(10):1988-93. DOI: https://doi.org/10.3174/ajnr.A4386.
9. Schabel C, Gatidis S, Bongers M, Hüttig F, Bier G, Kupferschlaeger J, et al. Improving CT-based PET attenuation correction in the vicinity of metal implants by an iterative metal artifact reduction algorithm of CT data and its comparison to dual-energy-based strategies: A phantom study. Invest Radiol. 2017;52(1):61-5. DOI: https://doi.org/10.1097/RLI.0000000000000306.
10. Martin O, Boos J, Aissa J, Vay C, Heusch P, Gaspers S, et al. Impact of different iterative metal artifact reduction (iMAR) algorithms on PET/CT attenuation correction after port implementation. Eur J Radiol. 2020;129:109065. DOI: https://doi.org/10.1016/j.ejrad.2020.109065.

11. Martin O, Aissa J, Boos J, Wingendorf K, Latz D, Buchbender C, et al. Impact of different metal artifact reduction techniques on attenuation correction in ^{18}F-FDG PET/CT examinations. Br J Radiol. 2020;93(1105):20190069. DOI: https://doi.org/10.1259/bjr.20190069.
12. Morawitz J, Martin O, Boos J, Sawicki LM, Wingendorf K, Sedlmair M, et al. Impact of different metal artifact reduction techniques on attenuation correction of normal organs in ^{18}F-FDG-PET/CT. Diagnostics (Basel). 2022;12(2):375. DOI: https://doi.org/10.3390/diagnostics12020375.
13. Reinert CP, la Fougère C, Nikolaou K, Pfannenberg C, Gatidis S. Value of CT iterative metal artifact reduction in PET/CT—clinical evaluation in 100 patients. Br J Radiol. 2019;92(1096):20180756. DOI: https://doi.org/10.1259/bjr.20180756.
14. Kim J, Kim JI, Lee HJ, Kim JE. Metal artifact SUV estimation by using attenuation correction image and non attenuation correction image in PET-CT. J Nucl Med Technol. 2016;20(2).
15. Lee MG, Park C. The feasibility of algorithm for iterative metal artifact reduction (iMAR) using customized 3D printing phantom based on the SiPM PET/CT scanner. Korean J Nucl Med Technol. 2024;28(1):35-40. DOI: https://doi.org/10.12972/kjnmt.20240006.
16. Moon SG, Hong SH, Choi JY, et al. Metal artifact reduction by the alteration of technical factors in multidetector computed tomography: A 3-dimensional quantitative assessment. J Comput Assist Tomogr. 2008;32(4):630-33. DOI: https://doi.org/10.1097/RCT.0b013e3181568b27.